PHYSICAL REVIEW D **95,** 043502 (2017)

Cosmological inference using only gravitational wave observations of binary neutron stars

Walter Del Pozzo*
School of Physics and Astronomy, University of Birmingham, Edgbaston, Birmingham B15 2TT, United Kingdom
Dipartimento di Fisica "Enrico Fermi", Università di Pisa, Pisa I-56127, Italy

Tjonnie G. F. Li
LIGO - California Institute of Technology, Pasadena, California 91125, USA
Department of Physics, The Chinese University of Hong Kong, Shatin, N.T., Hong Kong

Chris Messenger
SUPA, School of Physics and Astronomy, University of Glasgow, Glasgow G12 8QQ, United Kingdom
(Received 22 June 2015; published 2 February 2017)

Gravitational waves emitted during the coalescence of binary neutron star systems are self-calibrating signals. As such, they can provide a direct measurement of the luminosity distance to a source without the need for a cross-calibrated cosmic distance-scale ladder. In general, however, the corresponding redshift measurement needs to be obtained via electromagnetic observations since it is totally degenerate with the total mass of the system. Nevertheless, Fisher matrix studies have shown that, if information about the equation of state of the neutron stars is available, it is possible to extract redshift information from the gravitational wave signal alone. Therefore, measuring the cosmological parameters in pure gravitational-wave fashion is possible. Furthermore, the huge number of sources potentially observable by the Einstein Telescope has led to speculations that the gravitational wave measurement is potentially competitive with traditional methods. The Einstein Telescope is a conceptual study for a third generation gravitational wave detector which is designed to yield 10^3–10^7 detections of binary neutron star systems per year. This study presents the first Bayesian investigation of the accuracy with which the cosmological parameters can be measured using information coming *only* from the gravitational wave observations of binary neutron star systems by the Einstein Telescope. We find, by direct simulation of 10^3 detections of binary neutron stars, that, within our simplifying assumptions, H_0, Ω_m, Ω_Λ, w_0 and w_1 can be measured at the 95% level with an accuracy of ∼8%, 65%, 39%, 80% and 90%, respectively. We also find, by extrapolation, that a measurement accuracy comparable with current measurements by Planck is possible if the number of gravitational wave events observed is $O(10^{6-7})$. We conclude that, while not competitive with electromagnetic missions in terms of significant digits, gravitational waves alone are capable of providing a complementary determination of the dynamics of the Universe.

DOI: 10.1103/PhysRevD.95.043502

I. INTRODUCTION

The family of second generation interferometers Advanced LIGO [1] began its operations in the last quarter of 2015 [2]. Advanced Virgo [3] is scheduled to join the LIGO network in 2017, with KAGRA [4] and LIGO India [5] to follow afterwards. The detection of gravitational waves from the coalescence of merging black holes [6–8] has led already to important scientific measurements as tests of general relativity [8,9] and astrophysics [8,10,11]. Given the expected number of yearly detections [8,12,13], the expectations on the scientific deliverables are high: tests of the strong field dynamics of general relativity [8,9,14–16], a "cosmic distance scale ladder"-free determination of the Hubble constant [17–19], and a determination of the neutron star equation of state [20–23].

Detectors beyond the second generation are already being envisaged. For instance, the Einstein gravitational wave Telescope (ET) [24] is a proposed underground detector consisting of three 10 km arm length Michelson interferometers in a triangular topology with opening angles of 60 degrees [25]. The strain sensitivity is estimated as a factor of 10 better than second generation detectors, down to frequencies of 1–3 Hz depending on the actual configuration of the instrument [26]. The high sensitivity

*walter.delpozzo@unipi.it

promises the detection of a very large number of gravitational waves (GW) signals with large signal-to-noise ratios (SNR), thus allowing for unprecedented population studies as well as extremely accurate measurements of the physical parameters of coalescing binary systems [24].

A. Cosmological inference with gravitational waves

When estimating the parameters of GW sources, and in particular the coalescences of binary neutron stars and black holes, the luminosity distance can be observed directly [27,28]. This makes GW an ideal laboratory to place samples in the Hubble diagram in a manner that is free from the potential systematics affecting electromagnetic (EM) methods. Unfortunately, in the vast majority of cases, the redshift cannot be measured from GW alone and this piece of information needs to be extracted by means other than GW.

In recent years, various proposals have been put forward to overcome this difficulty. For instance, one can assume that the coalescences of compact binaries are the progenitors of short gamma ray bursts (sGRBs) [29]. In this case, coincident observations of a GW event and the correspondent sGRB would allow the measurement of the luminosity distance from GW and the redshift from spectroscopy of the host galaxy [17,30–32].[1] For second generation interferometers, this method indicates a relative accuracy on the measurement of the Hubble constant H_0 of a few percent in the case where 10–15 such events are detected. However, whether the coalescences of compact binaries are the progenitors of sGRBs is still a matter of debate. Also, the fraction of GW events also observable as sGRBs might be as low as 10^{-3} [35] due to sGRB beaming effects.

An alternative approach, following broadly the argument first given in Ref. [27], would be to statistically identify the possible host galaxies of a GW event to obtain a distribution of possible redshifts associated with each GW detection. This method should yield ∼5% percent accuracy on H_0 using 20–50 events [18] observed by Advanced LIGO/Virgo. A similar methodology has also been applied to space-based detectors [36,37].

A few methods aim at extracting the redshift using GW observations alone. For example, one can use the knowledge of the (rest frame) mass function of NS and the measured (redshifted) mass to infer the redshift of the source [19,38]. In this framework, second generation interferometers should infer the Hubble constant H_0 with ∼10% accuracy using about 100 events [19].

The results of advanced interferometers can be greatly improved by third generation instruments such as ET. In fact, ET can probe regions of the Universe where the effects of the dark energy will be substantial, thus allowing an independent sampling of the cosmic history.

The potentialities of ET have already been investigated by various groups [30,31,39], concluding that, when only a limited set of cosmological parameters is considered, the accuracy of the inference is comparable to that of current EM measurements.

B. Outline

In this paper, we will expand on the approach proposed by Messenger and Read [40] in which if one of the two components is a NS, information about the equation of state (EOS) allows a direct measurement of the rest-frame masses and thus of the source redshift [40]. Using Fisher matrix formalism, the authors estimate the accuracy with which z can be measured to be ∼8–40%, depending on the EOS and on the distance to the source. Recently, a similar investigation was carried out in [41] using a more realistic Monte Carlo data analysis method. The authors concluded that the average uncertainty is closer to 40% for a hard EOS and essentially independent of redshift.

Nevertheless, given the large number of sources that can be observed by ET and the possibility of combining information across them, even the large uncertainty reported in Ref. [41] could be sufficient to obtain interesting indications on the accuracy with which ET will measure the cosmological parameters. In this paper, we explore this idea in a simplified scenario and conclude that ET can indeed set bounds that are comparable to current EM measurement. We are interested in the cosmological information that can be inferred *exclusively* from the observation of gravitational waves. We will thus not discuss the potential of coincident GW-EM detections which are presented elsewhere [31,39]. We note here that, because of the colocation of the three ET interferometers and because of its topology, its expected sky resolution is extremely poor. Consequently, the probability of a successful EM-GW association is *a priori* very small. Note that at the time of ET, second generation detectors are expected to be operational with improved sensitivities [42]. For a substantial fraction of the loudest GW events, the sky localization from a network made of ET and advanced detectors will be vastly improved compared to ET alone. In this case, some of the aforementioned EM + GW methods might become feasible and used to yield constraints on the cosmological parameters.

The rest of the paper is organized as follows. In Sec. II we cast the problem in a Bayesian framework, and identify the necessary components to arrive at the cosmological inference. In Sec. III we describe the procedures of simulating GW events and the detector noise, and the implementation of the analysis. In Sec. IV we present the results of our simulations and finally in Sec. V we summarize and discuss our results. The mathematical solution to the problem of the inference of the cosmological parameters in the presence of a detection threshold is given for completeness in the Appendix.

[1]Kilonovae are also expected EM counterparts to binary neutron star (BNS) coalescences [33]. However their utility as cosmological probes is yet unclear due to their intrinsically faint luminosities (e.g. [34]) which limits the distance at which they can be confidently detected.

II. METHOD

In this section we present a Bayesian solution to the problem of computing posterior probability density functions for a set of cosmological parameters from GW data. We broadly follow the presentation in [18]. Note that the treatment is not specific to the case of ET.

A. Inference of the cosmological parameters in the absence of a detection threshold

Consider a catalogue of GW events $\mathcal{E} \equiv \{\epsilon_1, \ldots, \epsilon_N\}$. Each event is defined as a stretch of data $d_i(t)$ given by the sum of noise $n_i(t)$ and a gravitational wave signal $h_i(\vec{\Theta}_i; t)$, i.e.

$$\epsilon_i\colon\ d_i(t) = n_i(t) + h_i(\vec{\Theta}_i; t), \tag{1}$$

where $\vec{\Theta}_i$ indicates the set of all parameters of the signal i.

The noise is taken to be a stationary Gaussian process with a zero mean and covariance defined by its one-sided spectral density $S_n(f)$ such that

$$\begin{aligned} p(n_i|\mathrm{I}) &\propto \exp\left\{-\frac{1}{2}\int_0^\infty \mathrm{d}f 4\frac{|\tilde{n}_i(f)|^2}{S_n(f)}\right\}, \\ &\propto \exp\left\{-\frac{1}{2}(n|n)\right\} \end{aligned} \tag{2}$$

where I represents all the relevant information for the inference problem, a tilde represents the Fourier transform, and where we have introduced a scalar product between two real functions $A(t)$ and $B(t)$ as

$$(A|B) = 4\Re\int_0^\infty \mathrm{d}f \frac{\tilde{A}^*(f)\tilde{B}(f)}{S_n(f)}. \tag{3}$$

The likelihood of observing the event ϵ_i is then given by

$$p(\epsilon_i|\vec{\Theta}_i, \mathrm{S}, \mathrm{I}) \propto \exp\left\{-\frac{1}{2}(d_i - h_i|d_i - h_i)\right\} \tag{4}$$

where S is the signal model that relates the signal parameters $\vec{\Theta}_i$ to a gravitational wave signal h. Moreover, the signal-to-noise ratio (SNR) ρ can be succinctly written as

$$\rho = \sqrt{(h|h)}. \tag{5}$$

The posterior distribution for any parameter in our signal model S is related to the likelihood in Eq. (4) through the application of Bayes' theorem

$$p(\vec{\Theta}_i|\epsilon_i, \mathrm{S}, \mathrm{I}) \propto p(\vec{\Theta}_i|\mathrm{S}, \mathrm{I})\, p(\epsilon_i|\vec{\Theta}_i, \mathrm{S}, \mathrm{I}) \tag{6}$$

where $p(\vec{\Theta}_i|\mathrm{S}, \mathrm{I})$ is the prior probability distribution for the parameters $\vec{\Theta}_i$. When multiple independent detectors are included in the analysis, the likelihood [Eq. (4)] generalizes to

$$p(\epsilon_i|\vec{\Theta}_i, \mathrm{S}, \mathrm{I}) = \prod_k p(\epsilon_i^{(k)}|\vec{\Theta}_i, \mathrm{S}, \mathrm{I}). \tag{7}$$

For this work, we are only interested in the posterior probability for a subset of parameters $\vec{\Omega} \equiv \{H_0, \Omega_m, \Omega_\Lambda, \ldots\}$. Therefore, we marginalize over the remaining subset of parameters $\vec{\theta}_i$, i.e.

$$\begin{aligned} p(\vec{\Omega}|\epsilon_i, \mathrm{S}, \mathrm{I}) &= \int \mathrm{d}\vec{\theta}_i\, p(\vec{\Theta}_i|\epsilon_i, \mathrm{S}, \mathrm{I}) \\ &= \int \mathrm{d}\vec{\theta}_i\, p(\vec{\theta}_i, \vec{\Omega}|\mathrm{S}, \mathrm{I})\, p(\epsilon_i|\vec{\theta}_i, \vec{\Omega}, \mathrm{S}, \mathrm{I}) \\ &= p(\vec{\Omega}|\mathrm{S}, \mathrm{I}) \int \mathrm{d}\vec{\theta}_i\, p(\vec{\theta}_i|\vec{\Omega}, \mathrm{S}, \mathrm{I})\, p(\epsilon_i|\vec{\theta}_i, \vec{\Omega}, \mathrm{S}, \mathrm{I}) \\ &= p(\vec{\Omega}|\mathrm{S}, \mathrm{I})\mathcal{L}(\epsilon_i, \vec{\Omega}), \end{aligned} \tag{8}$$

where we have introduced the so-called "quasi-likelihood" [43]

$$\mathcal{L}(\epsilon_i, \vec{\Omega}) \equiv \int \mathrm{d}\vec{\theta}_i\, p(\vec{\theta}_i|\vec{\Omega}, \mathrm{S}, \mathrm{I})\, p(\epsilon_i|\vec{\theta}_i, \vec{\Omega}, \mathrm{S}, \mathrm{I}). \tag{9}$$

Finally, the posterior for $\vec{\Omega}$ given an ensemble of events $\mathcal{E}$ can be shown to be

$$p(\vec{\Omega}|\mathcal{E}, \mathrm{S}, \mathrm{I}) = p(\vec{\Omega}|\mathrm{S}, \mathrm{I}) \prod_i \mathcal{L}(\epsilon_i, \vec{\Omega}). \tag{10}$$

Therefore, in order to obtain the posterior for $\vec{\Omega}$, we need to perform a multidimensional integral in Eq. (9) for each of the GW events. The description of this procedure and the generation of data follow in Sec. III.

III. ANALYSIS

In this section we describe the simulation that was performed. Firstly, we outline the generation of the data, consisting of the GW signal model, the astrophysical and cosmological assumptions regarding the source population, and the simulation of the detector noise. Secondly, we show the data analysis implementation with which the simulated data were analyzed. In particular, we describe the construction of the quasi-likelihood, and it subsequent use to arrive at our cosmological inference. The GW signals and the detector noise have been generated using the LIGO Analysis Library (LAL) [44].

A. Astrophysical and cosmological assumptions

The NS masses are distributed according to a Gaussian distribution with a mean of $1.35M_\odot$ and a standard deviation of $0.15M_\odot$ [45] which is assumed constant throughout the cosmic history. For the NS equation of state we consider three cases: a hard EOS, a medium and a soft EOS. They are labeled as MS1 [46], H4 [47]

and SQM3 [48]. We investigate these three cases since in [40] it was shown that the accuracy with which the redshift can be measured depends on the magnitude of the physical effects related to the details of the EOS. One can think of these three cases as an optimistic, a realistic and a pessimistic one, respectively.

The events are distributed uniformly in the cosine of the inclination, polarization and time of arrivals. The events are also uniformly distributed in comoving volume. Their redshifts are sampled from the probability density given by [49]

$$p(z|\vec{\Omega}) = \frac{\mathrm{d}R(z)}{\mathrm{d}z}\frac{1}{R(z_{\max})} \tag{11}$$

where $R(z)$ is the cosmic coalescence rate. It is worth nothing that $p(z|\vec{\Omega})$ is an explicit function of $\vec{\Omega}$. The differential cosmic coalescence rate is equal to

$$\frac{\mathrm{d}R(z)}{\mathrm{d}z} = \frac{\mathrm{d}V}{\mathrm{d}z}\frac{r_0 e(z)}{1+z} \tag{12}$$

where r_0 is the local rate, $e(z)$ is the cosmic star formation rate and V is the comoving volume. In a Friedmann-Lemaître-Robertson-Walker (FLRW) universe, the rate of change of V with z is given by

$$\frac{\mathrm{d}V}{\mathrm{d}z} = 4\pi\frac{D_L^2(z)}{(1+z)^2 H(z)}, \tag{13}$$

where we have introduced the Hubble parameter

$$H(z) = H_0\sqrt{\Omega_m(1+z)^3 + \Omega_k(1+z)^2 + \Omega_\Lambda E(z, w(z))} \tag{14}$$

and the *luminosity distance* [50]

$$D_L(z) = \begin{cases} \frac{(1+z)}{\sqrt{\Omega_k}}\sinh\left[\sqrt{\Omega_k}\int_0^z \frac{dz'}{H(z')}\right] & \text{for } \Omega_k > 0 \\ (1+z)\int_0^z \frac{dz'}{H(z')} & \text{for } \Omega_k = 0\,. \\ \frac{(1+z)}{\sqrt{|\Omega_k|}}\sin\left[\sqrt{|\Omega_k|}\int_0^z \frac{dz'}{H(z')}\right] & \text{for } \Omega_k < 0 \end{cases} \tag{15}$$

H_0 is the Hubble constant, Ω_m is the matter fractional density, Ω_Λ is the fractional energy density of dark energy, and $\Omega_k = 1 - \Omega_m - \Omega_\Lambda$ is the curvature. Finally

$$E(z, w(z)) = (1+z)^{3(1+w_0+w_1)} e^{-3w_1 z/(1+z)} \tag{16}$$

is a convenient parametrization to capture the effects of the redshift evolution of dark energy [51]. For $\vec{\Omega}$ we chose fiducial values of

$$(h, \Omega_m, \Omega_\Lambda, \Omega_k, w_0, w_1)^{\mathrm{fid}} = (0.7, 0.3, 0.7, 0, -1, 0), \tag{17}$$

where $h = H_0/100\ \mathrm{km\,Mpc^{-1}\,s^{-1}}$. Even though the ET horizon distance is $\simeq$37 Gpc ($z \simeq 4.15$ for our fiducial cosmology), we limit our analysis to $z_{\max} = 2$ as this corresponds approximately to the sky averaged horizon distance of 13 Gpc for BNS systems [52]. For simplicity, we decided to assume a star formation rate $e(z)$ that does not change with redshift and is therefore irrelevant for our problem.

We simulated 1,000 binary NS events as observed by ET. The parameters θ_i of each individual source have been generated according to the assumptions described in Sec. III A. The corresponding waveform $\tilde{h}(f, \vec{\Theta}_i)$ was then added to Gaussian noise which is colored according to the amplitude spectral density shown in Fig. 2. In Fig. 1 we show the network SNR distribution in the ET detector computed using Eq. (5).

Differently from most existing literature, we do not filter our sources with any SNR threshold. If we were to do so, we would be introducing a selection bias [53]. Note that, due to the potentially large number of sources observed by ET and their distribution in a comoving volume, the vast majority of them will in practice not be detected in a search which uses the SNR as decision statistics. It is known that ignoring these unregistered sources leads to a significant bias in the estimation of "global" parameters; see [53].

The main reason for the emergence of biases is intimately linked to the functional form for the prior on z, Eq. (11). Since Eq. (11) quantifies the prior expectation regarding the distribution of sources in the comoving volume, it is an explicit function of $\vec{\Omega}$. The quasi-likelihoods for the majority of our simulated events are almost uniform in $\vec{\Omega}$ (see Sec. III C 2); therefore our inference is greatly influenced by the prior distribution: if one were to analyze sources that are louder than some threshold SNR the overall population of events would appear on average

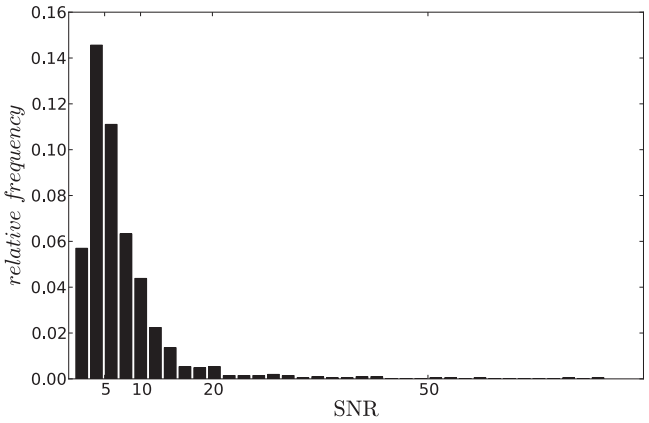

FIG. 1. Network SNR distribution of the 1,000 BNS events generated sampling Eqs. (11) and (13) for a our fiducial cosmology Eq. (17).

closer than the actual population. At the same time, the observed distribution of z would follow the actual cosmological distribution. Since $p(z|\vec{\Omega})$ in Eq. (11) relates D_L and z via $\vec{\Omega}$, this leads to estimates of $\Omega_m \to 1$ and $h \to 0$. Similarly, if one were to consider only events that are quieter than a given SNR threshold, then $\Omega_m \to 0$ and $h \to 1$, and thus $\Omega_\Lambda \to 1$. In the Appendix, we give a mathematical solution to the problem of inferring $\vec{\Omega}$ that accounts for sets of unobserved events. However, the solution in the Appendix is not computationally treatable with current techniques and for a large number of events; therefore we opted for a SNR selection threshold of 0 and analyzed all simulated events. Furthermore, our choice relies on the capacity of distinguishing between low SNR GW signals and low SNR background events due to noise in the detector. A discussion of this problem can be found in [53]. The triangular configuration of ET provides an additional tool to study the distribution of signal and noise in low SNR events. Thanks to its topology, ET admits the construction of a null stream which is devoid of any GW signal as the sum of the outputs of the individual Michelson detectors [25]. Being a pure noise process, the analysis of the null stream can be used to understand the SNR distribution of noise events which can then be used to infer the SNR distribution of quiet sources.

B. The signal model

In the previous paragraph we introduced the signal model S without specifying its properties. In this section, we lay out the assumptions that go into the construction of S.

In modeling the GW from a binary system, we limit our analysis to the inspiral phase of the coalescence process. We model the inspiral using an analytical frequency domain 3.5 post-Newtonian waveform in which we ignore amplitude corrections and the effects of spins. This is not a big limitation as NS are expected to be slow rotators [54]. In particular, we use the so-called TaylorF2 approximant [55], which can be written as

$$\tilde{h}(\vec{\Theta}; f) = A(\vec{\Theta}) f^{-7/6} e^{i\Phi(\vec{\Theta};f)}, \tag{18}$$

where the waveform is written in terms of the amplitude $A(\vec{\Theta})$ and the phase $\Phi(\vec{\Theta}; f)$.

The amplitude of the waveform $A(\vec{\Theta})$ is given by

$$A(\vec{\Theta}) \propto \frac{\mathcal{M}^{5/6}}{D_L} Q(\iota, \psi, \alpha, \delta) \tag{19}$$

where we have introduced the chirp mass $\mathcal{M} = m_1^{3/5} m_2^{3/5}/(m_1 + m_2)^{1/5}$; D_L is the luminosity distance defined in Eq. (15); (α, δ) signify the sky position of the source; and (ι, ψ) give the orientation of the binary with respect to the line of sight [55].

The wave phase can be written in the form

$$\Phi(\vec{\Theta}; f) = 2\pi f t_c - \phi_c - \frac{\pi}{4} + \sum_{n=0}^{7} [\psi_n + \psi_n^{(l)} \ln f] f^{(n-5)/3}, \tag{20}$$

where the ψ_n are the so-called post-Newtonian coefficients (see e.g. [56]), which are functions of the component masses m_1 and m_2, and (t_c, ϕ_c) are the time and phase of coalescence. Note that all masses are defined in the observer frame, and the rest frame mass $m_{\rm rest}$ is related to the observed mass through

$$m = m_{\rm rest}(1 + z), \tag{21}$$

where z is the redshift of the GW source.

The description of the phase in Eq. (20) assumes that the object is a point particle, and thus cannot be tidally deformed. However, since we consider all of our events are binary NS coalescences, we modify the gravitational wave phase in Eq. (20) by including the finite-size contributions to the phase. These in turn depend on the *tidal deformability* $\lambda(m_{\rm rest})$ [21] of the star which is a function of its equation of state and its rest frame mass. The finite-size contributions to the GW phase, as a function of observed masses, are given by

$$\Phi_{\rm tidal}(\vec{\Theta}; f) = \sum_{a=1}^{2} \frac{3\lambda_a (1+z)^5}{128\eta M^5} \left[-\frac{24}{\chi_a}\left(1 + \frac{11\eta}{\chi_a}\right)(\pi M f)^5 - \frac{5}{28\chi_a}(3179 - 919\chi_a - 2286\chi_a^2 + 260\chi_a^3)(\pi M f)^7 \right], \tag{22}$$

where the sum is over the components of the binary, $\chi_a = m_a/M$, $\lambda_a = \lambda(m_a)$ where m_a are the component masses, M is the total mass, and $\eta = m_1 m_2/M^2$.

Knowledge of the EOS and using information encoded in the GW tidal phase contribution allows us to measure the redshift of the source [40]. While the EOS is not known yet, various studies have shown that it could be possible to infer it from observations of BNS with second generation detectors [20–23,57,58]. In what follows, we will assume that the nature of the NS interior is known.

C. Data analysis

For our analysis, we assumed a noise curve for ET corresponding to the "B" configuration [59], corresponding to the projected sensitivity achievable with the current technologies (see Fig. 2). Given the anticipated rates of compact binary coalescences [13], the detection rates of binary NS systems in ET are expected to lie in the range 10^3–10^7 yr^{-1} [24].

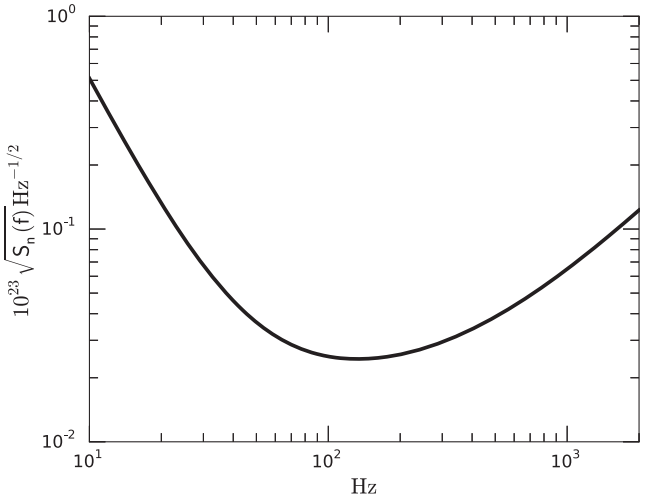

FIG. 2. Amplitude spectral density for ET in the "B" configuration.

The parameters $\vec{\theta}$ of our signal model are the component masses m_1 and m_2, inclination ι, polarization ψ, right ascension α and declination δ, the time of coalescence t_c, the phase of coalescence ϕ_c, luminosity distance D_L and the redshift z. In our analysis we ignored the presence of spins, as it is believed to be small in binary NS systems [54]. We analyzed our ensemble of sources assuming that the EOS of the NS is known, thus accounting for a total of three analysis runs (one for each of our predefined hard, medium and soft EOSs). To obtain the posterior probability distribution on the cosmological parameters $\vec{\Omega}$ we proceeded in three steps. Firstly, we analyzed each source to compute a quasi-likelihood as a function of the redshift z and the luminosity distance D_L. Secondly, these quasi-likelihoods are then converted into quasi-likelihoods as a function of the cosmological parameters $\vec{\Omega}$ as shown in Eq. (9). Finally, the posterior probability function for the cosmological parameters given an ensemble of events is computed from Eq. (10).

1. Obtaining the quasi-likelihood

For each event ϵ_i, we compute the quantity

$$\mathcal{L}(\epsilon_i, D_L, z, \vec{\Omega}) \equiv \int \mathrm{d}\vec{\lambda}\, p(\vec{\lambda}|\vec{\Omega}, \mathrm{S}, \mathrm{I})\, p(\epsilon_i|\vec{\lambda}, \vec{\Omega}, \mathrm{S}, \mathrm{I}) \qquad (23)$$

that is a partially marginalized quasi-likelihood, where the marginalization is done on all parameters that are not relevant to the inference of $\vec{\Omega}$. These are $\vec{\lambda} \equiv (m_1, m_2, \psi, \iota, \phi_c, t_c, \alpha, \delta)$. The further marginalization over z and D_L will be described later on. For the time being, let us describe the details of the analysis for the computation of Eq. (23). The above integral was computed using a nested sampling algorithm [60] implemented similarly to what was described in [61]. For each of the three analysis runs, we chose the same prior probability distributions for all parameters, with the exception of the component masses. For the common parameters we used uniform probability distributions on the 2-sphere for sky position (α, δ) and orientation (ψ, ι) and uniform in the time of coalescence t_c with a width of 0.1 seconds around the actual coalescence time. For the first marginalization, we choose uniform sampling distributions for both D_L and z in the intervals [1, 10^5] Mpc and [0,2], respectively.

For the component masses, the priors were different across the different runs; each EOS in fact predicts not only the functional form of the tidal deformability $\lambda(m)$ that enters in the phase of the GW waveform, but also the maximum permitted mass of the NS itself. Therefore, for the three EOSs under consideration we used the maximum expected rest frame mass M_{max} of 2.8, 2.0, $2.0M_\odot$ for MS1, H4 and SQM3 respectively. The prior probability distribution for the component masses was then chosen to be uniform between $1M_\odot$ and M_{max}.

2. Cosmological inference

The marginalization over the redshift and luminosity distance was then performed as follows: once a cosmological model is introduced, z and D_L are not independent parameters anymore; they are related unequivocally by Eq. (15). Thus—after some algebra which can be found in [18]—we are left with the following integral to compute,

$$\mathcal{L}(\epsilon_i, \vec{\Omega}) = \int_0^{z_{\mathrm{max}}} \mathrm{d}z\, p(z|\vec{\Omega}, \mathrm{SI})\, \mathcal{L}(\epsilon_i, D_L(z), z, \vec{\Omega}), \qquad (24)$$

where $p(z|\vec{\Omega}, \mathrm{SI})$ is given in Eq. (11) and we choose, consistently with the source's generation, $z_{\mathrm{max}} = 2$.

One of the problems we needed to overcome in order to perform the integral in Eq. (24) was how to represent $\mathcal{L}(\epsilon_i, D_L(z), z, \vec{\Omega})$ in a tractable way. In fact, one of the outputs of the nested sampling algorithm is a set of samples drawn from the integrand in Eq. (23) which is difficult to manipulate—in particular difficult to integrate—without making any assumptions about the underlying probability distribution.

A possible treatment of the problem would be to use the samples from Eq. (23) and approximate it using a normalized histogram. This procedure was successfully used in other unrelated studies [14]; however, for our purposes it is not accurate enough. In fact, a histogram representation is dependent on a parameter, the bin size (or equivalently the number of bins once the range is specified), which cannot be inferred from the data but has to be chosen arbitrarily. The majority of the quasi-likelihoods in Eq. (24) tend to be very uniform over the cosmological parameter space for individual sources and, as noted in Sec. III A, the inference is strongly dominated by the prior on z. Most sources are close to or below the detection threshold of the detector. Thus a single source, in general, yields very little information about the underlying cosmology. Therefore any small fluctuation in the histogram approximation due to the random variation of

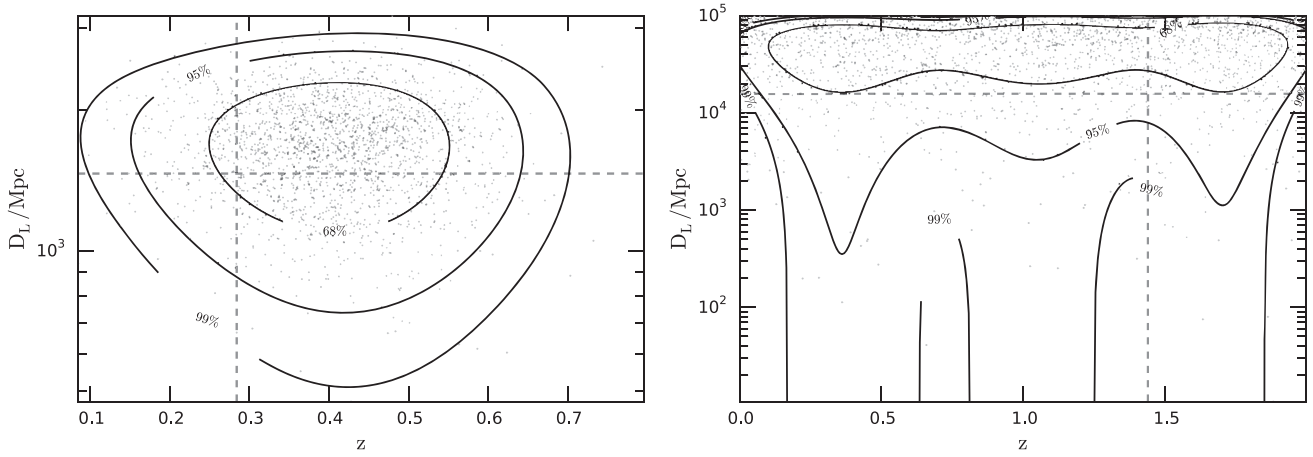

FIG. 3. Sample marginal likelihoods [Eq. (23)] for z and D_L. The left panel shows the marginal likelihood for an event with a network SNR $= 25$. The right panel shows the marginal likelihood for an event with a network SNR $= 4$. On both panels, the lines indicate the source distance and redshift.

the number of samples in any specific bin would be amplified and would eventually lead to a biased estimate of the posterior probability density for $\vec{\Omega}$. As an example, compare the panels in Fig. 3. The left panel shows samples from Eq. (24) for a source having a network SNR $= 25$. In this case, the isoprobability contours are almost consistent with a normal distribution. The right panel shows instead a source with network SNR $= 4$. In this case the samples are almost uniformly distributed; thus if one were to approximate Eq. (24) with a two-dimensional histogram, different choices of the bin size would result in different approximations, which would yield very different inferences of $\vec{\Omega}$. Instead, we decided to follow a different course of action. Given a set of samples, for *any* partition of the parameter space, the resulting probability distribution of the observations is always a multinomial distribution; therefore the "probability distribution" of the occurrences in each bin is a Dirichlet distribution. The above property defines a Dirichlet process [62] which can be used to define an analytical representation of the underlying probability distribution of which we have only a finite number of samples available. For the mathematical details and definitions, the reader is referred to the original paper by Ferguson [62] or to the more recent discussions in [63]. We used the approximate variational algorithm [64] as implemented in [65] to find the Dirichlet process Gaussian mixture model to represent the integrand in Eq. (24). The output of this procedure is an analytical representation of the target probability distribution as an infinite mixture of Gaussian distributions which is analytical and continuous. This form can then be used as the integrand in Eq. (24) and the integral itself can be evaluated using another nested sampling algorithm whose output can then be combined to compute the posteriors for $\vec{\Omega}$, Eq. (10).

For this last marginalization, we assume priors on $\vec{\Omega}$ that are uniform in all parameters. In particular, $h \in [0.1, 1.0]$, $\Omega_m \in [0.0, 1.0]$, $\Omega_\Lambda \in [0.0, 1.0]$, $w_0 \in [-2, 0]$ and finally $w_1 \in [-1, 1]$.

IV. RESULTS

For each of the equations of state assumed we considered various scenarios within the set of $(h, \Omega_m, \Omega_\Lambda, w_0, w_1)$. We show posterior distributions for the cosmological parameters obtained from the joint analysis of 1,000 events.

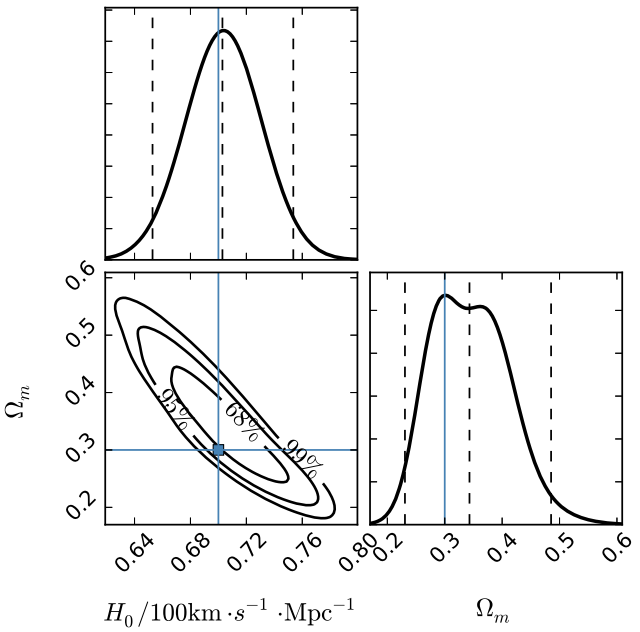

FIG. 4. Posterior distributions for h and Ω_m obtained from the analysis of 1,000 BNS events for a flat universe ($\Omega_k = 0$) and no dark energy equation of state. In the one-dimensional posteriors the dashed lines indicate the 2.5%, 50% and 97.5% confidence levels. In the two-dimensional posterior distribution we show the 68%, 95% and 99% confidence regions. On all panels the solid (blue) lines indicate the fiducial values.

We also report confidence intervals from the number of events greater than 1,000 obtained via extrapolation.

Moreover, since all EOSs yield very similar results, we choose to report only posteriors for the cosmological parameters obtained from the MS1 equation of state.

We computed posterior distribution functions for three distinct cases:

(i) flat FLRW universe, Fig. 4;
(ii) general FLRW universe, Fig. 5;
(iii) general FLRW universe, with dark energy parameters, Fig. 6.

In the following subsections we report on the values of the various cosmological parameters in each different cosmological model we considered. We note here that, as expected, the accuracy of the cosmological parameters measurement is better for the flat case and gets progressively worse with the increasing dimensionality of the model under consideration. Also, all uncertainties we report are at the 95% confidence level.

Posterior distributions on the parameters of all cosmological models from the analysis of 10^3 BNS events are reported in Figs. 4, 5 and 6.

Depending on the actual astrophysical rate, ET will observe between 10^3 and 10^7 BNS events per year [24]. It is computationally unfeasible at the moment to simulate and analyze in a realistic way such a large number of events. We therefore extrapolated the results we obtained for 1,000 sources to the maximum expected number of events. We assumed that the central limit theorem holds; in other words that our posteriors for 10^3 events are approximately Gaussian, and simply scaled the variance of the one-dimensional posteriors by the number of sources N. Tables I, II and III show the extrapolation of the 95% widths (2σ) to a number of events ranging from 10^4 to 10^7 for all relevant parameters for each of the cosmological models we considered in our analysis.

A. H_0

We find that 10^3 BNS observations yield the following results: for the model (i) the accuracy is 0.05 (7%) which remains approximately constant in the case (ii) and worsens to 0.08 (11%) in the general case (iii). In comparison with other GW studies, we find our measurements to be significantly worse. For instance [18] reports a 95% accuracy of ∼10% with second generation interferometers and similarly so do [32] and [38]. In comparison to traditional methods, the most constraining measurement from the Planck experiment in conjunction with other methods reports an accuracy of ∼0.5% [66]. So with 10^3 GW sources current measurements are far more accurate

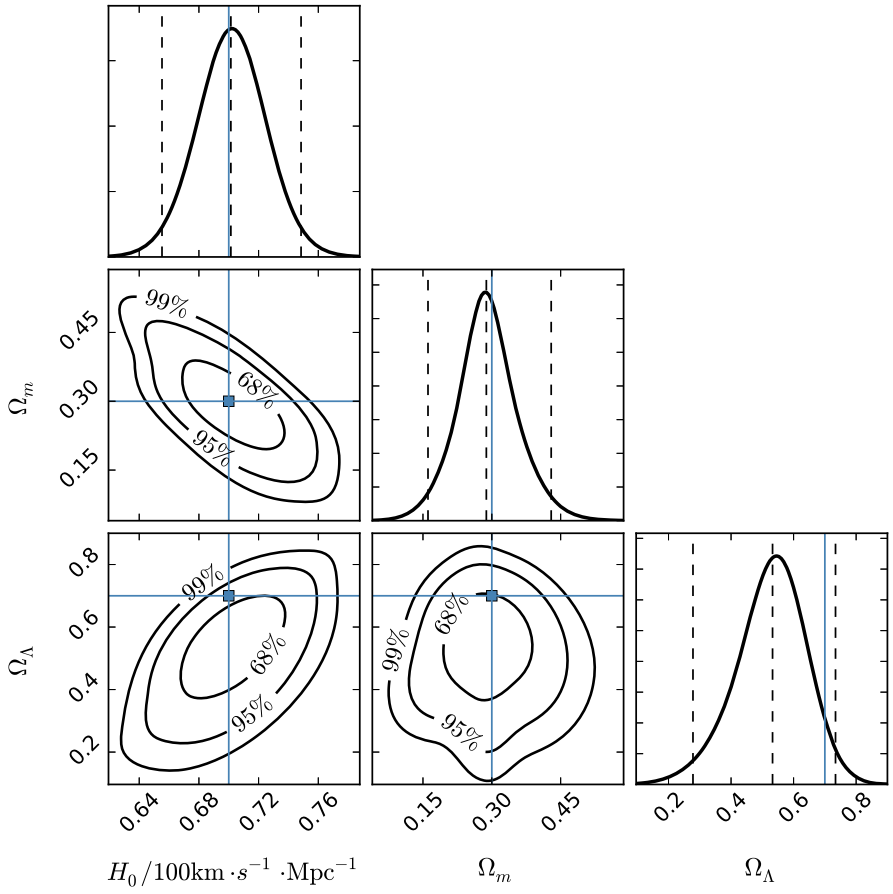

FIG. 5. Same as Fig. 4, but for a general FLRW universe.

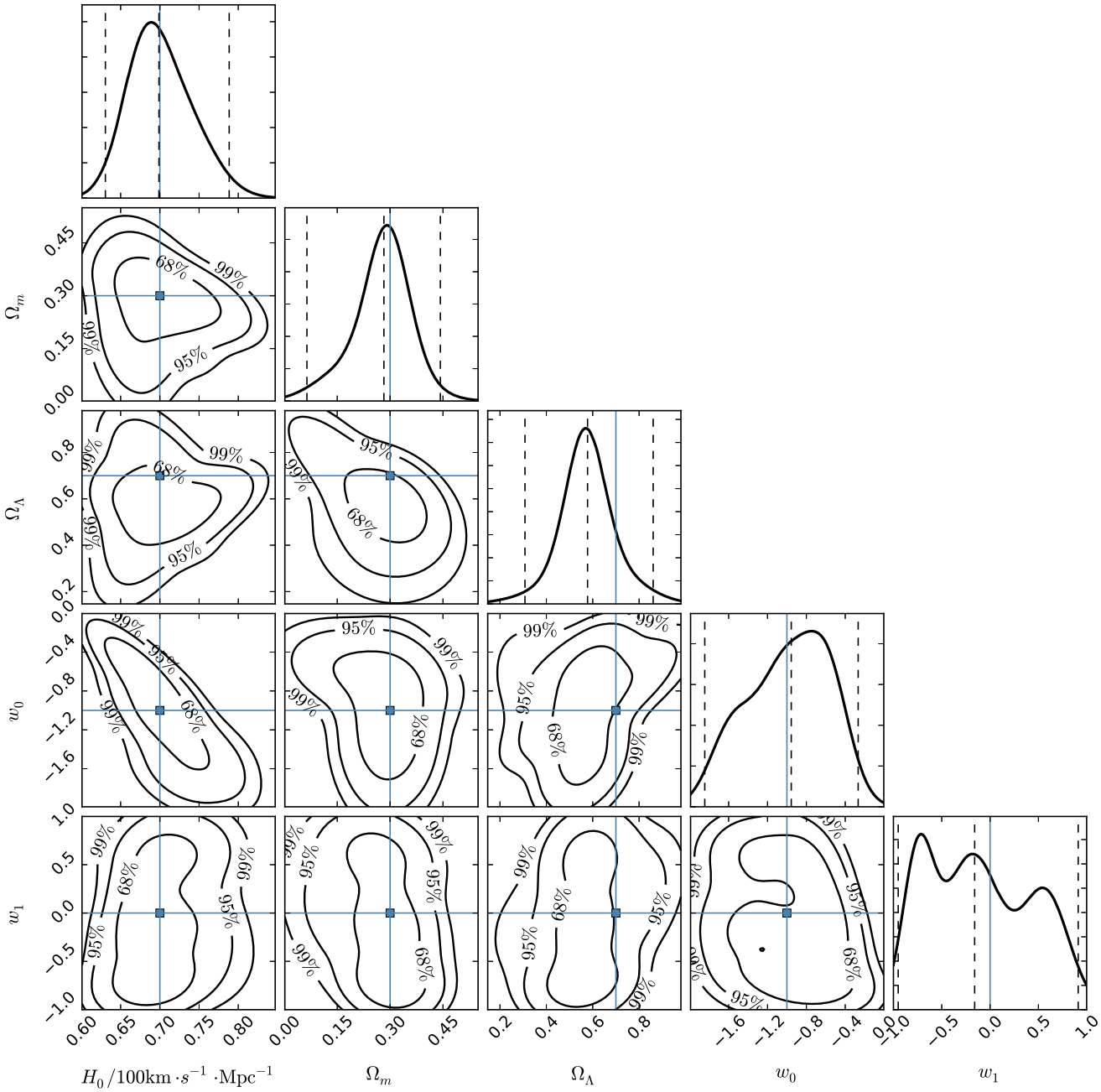

FIG. 6. Same as Fig. 4, but for a general FLRW universe + DE parameters.

than those obtained with our method using ET. However, when extrapolating to the potential number of observable BNS systems, we find the Planck-like accuracy is reached with $\sim 10^5$ BNS observations. A further order of magnitude improvement is seen for 10^7 BNS observations; see Table I.

B. Ω_m and Ω_Λ

We find that with 10^3 BNS events Ω_m can be measured with an accuracy of 0.125 (47.5%), 0.135 (45%) and 0.19 (65.5%) for the models (i), (ii) and (iii) respectively. The above numbers compare very unfavorably with the ∼2% yield by Planck [67]. However, if more sources are observed the current accuracy is reached with 10^{6-7} sources, depending on the actual cosmological model.

The situation is similar for the measurement of the cosmological constant Ω_Λ. With 10^3 BNS observations we find an accuracy of 0.23 (37.5%) and 0.275 (39%) for the models (ii) and (iii) respectively. As a comparison Planck reports ∼0.9% [66]. However, a similar uncertainty is reached with 10^{6-7} sources. The results are summarised in Table II.

C. Dark energy parameters

In the case in which the $D_L - z$ relation is modified to allow for a time varying cosmological constant

TABLE I. 95% accuracies on the measurement of the reduced Hubble parameter for various detected numbers of sources for the general five parameter case. For 10^3 sources, the widths have been computed using our nested sampling algorithm; otherwise the widths are the result of an extrapolation.

	Δh				
	N				
Model	10^3	10^4	10^5	10^6	10^7
Flat FLRW	0.5×10^{-1}	1.6×10^{-2}	0.5×10^{-2}	1.6×10^{-3}	0.5×10^{-3}
General FLRW	4.6×10^{-2}	1.5×10^{-2}	4.6×10^{-3}	1.5×10^{-3}	4.6×10^{-4}
General FLRW + DE	0.8×10^{-1}	2.5×10^{-2}	0.8×10^{-2}	2.5×10^{-3}	0.8×10^{-3}

TABLE II. 95% accuracies on the measurement of the matter energy density Ω_m and the cosmological constant Ω_Λ for various detected numbers of sources for the general five parameter case. For 10^3 sources, the widths have been computed using our nested sampling algorithm; otherwise the widths are the result of an extrapolation.

	$\Delta\Omega_m$				
	N				
Model	10^3	10^4	10^5	10^6	10^7
Flat FLRW	1.3×10^{-1}	4.0×10^{-2}	1.3×10^{-2}	4.0×10^{-3}	1.3×10^{-3}
General FLRW	1.3×10^{-1}	4.2×10^{-2}	1.3×10^{-2}	4.2×10^{-3}	1.3×10^{-3}
General FLRW + DE	1.9×10^{-1}	0.6×10^{-1}	1.9×10^{-2}	0.6×10^{-2}	1.9×10^{-3}
	$\Delta\Omega_\Lambda$				
	N				
Model	10^3	10^4	10^5	10^6	10^7
General FLRW	2.3×10^{-1}	0.7×10^{-1}	2.3×10^{-2}	0.7×10^{-2}	2.3×10^{-3}
General FLRW + DE	2.8×10^{-1}	0.9×10^{-1}	2.8×10^{-2}	0.9×10^{-2}	2.8×10^{-3}

TABLE III. 95% accuracies on the measurement of the dark energy parameters w_0 and w_1 for various detected numbers of sources. For 10^3 sources, the widths have been computed using our nested sampling algorithm; otherwise the widths are the result of an extrapolation.

	Δw_0				
	N				
Model	10^3	10^4	10^5	10^6	10^7
General FLRW + DE	0.8×10^{0}	2.5×10^{-1}	0.8×10^{-1}	2.5×10^{-2}	0.8×10^{-2}
	Δw_1				
	N				
Model	10^3	10^4	10^5	10^6	10^7
General FLRW + DE	0.9×10^{0}	2.9×10^{-1}	0.9×10^{-1}	2.9×10^{-2}	0.9×10^{-2}

[see Eq. (16)], the parameters w_0 and w_1 were included in the model. From the analysis of 10^3 events, at 95% confidence, we find $\Delta w_0 = 0.8$ and $\Delta w_1 = 0.9$. In comparison, assuming 10^3 BNS events with optical counterparts and electromagnetic priors on the remaining cosmological parameters [31] finds $\Delta w_0 \approx 0.1$ and $\Delta w_1 = 0.3$. The most recent determination by Planck [67] of the parameters w_0 and w_1 reports $\Delta w_0 \approx 0.2$ and $\Delta w_1 \approx 0.5$. Extrapolation to the potential number of sources observable in 1 year shows that the accuracy on w_0 and w_1 can be improved by 2 orders of magnitude, thus 1 order of magnitude better than the current best estimates; see Table III. It is worth noting that the posterior distributions for w_0 and w_1 are not very Gaussian; therefore the extrapolations to a large number of events might not be as reliable as for the other cosmological parameters.

V. DISCUSSION

In this study we investigated the potentialities of BNS observations with ET as cosmological probes. In particular, we quantified the cosmological information that can be extracted from pure GW observations of BNS. The ingredient that allows the measurement of the redshift is the knowledge of the NS equation of state and thus of the NS tidal deformability.

We simulated 1,000 events and relied on extrapolation to the expected 10^4–10^7 events per year. The main result of this study is that from GW alone, ET could measure all cosmological parameters with an accuracy that is comparable with current state-of-the-art measurements from EM missions.

This is the very first study of this kind, and therefore it should be regarded as a proof of principle. Our analysis relies on a set of simplifying assumptions which should be progressively relaxed for a comprehensive investigation. We neglected the NS spins and eventual precession of the orbital plane. We do not expect this to be a serious limitation, since NSs are expected to be slow rotators [54]; however it is not clear how a small degree of precession would impact the analysis of ET data. There is evidence that for binary black holes and NS black hole binaries accounting for precession of the orbital plane leads to more accurate distance measurements [68]. If a redshift measurement can be associated to these classes of sources, the determination of $\vec{\Omega}$ would improve substantially, also thanks to the considerably larger volume that is observable by ET.

Due to its low frequency sensitivity, BNS signals in the local Universe ($z < 1$) will be in the ET sensitive band for a time scale of hours to days, depending on the observer frame masses. It is clear that this problem cannot currently be investigated using a fully realistic simulation since the generation of the most accurate waveforms and cutting edge data analysis algorithms are not yet sufficiently fast. A further complication arises from the number of signals itself; a detection rate of 10^7 events per year implies an average time delay between signals of ∼3 seconds. Given the duration of the signals in the band, it follows that several signals would be present simultaneously in the ET data stream at any given time. No systematic study or algorithm yet exists to investigate this problem.

We further assumed perfect knowledge of the NS EOS. While there are indications that second generation interferometers could measure the EOS [20–23], it is unlikely that we would know it without any form of uncertainty. However, we do not consider this a serious limitation as long as the error bar on any given value of the NS mass m and its tidal deformability $\lambda(m)$ is sufficiently small to avoid confusion between different EOSs. Moreover, we did not include in our analysis the merger part of the waveform, which, especially for the most distant sources, would be in the sensitive band of ET. The inclusion of the merger in the analysis would yield more information about the BNS mass and spin parameters as well as introducing a possible further constraint on the BNS redshift [69], allowing for more precise measurements.

A further element that deserves future investigation is the effect of detection thresholds. We give a formal solution to the problem of the inference of the cosmological parameters in the Appendix. However, we did not explore the details of its practical implementation, which we defer to a future study.

We ignored the effects of the detector calibration uncertainties over the inference of the GW event parameters as well as their impact over the global inference of $\vec{\Omega}$. At the end of the first observing run of Advanced LIGO, typical amplitude uncertainties (which are relevant for the determination of D_L) and phase uncertainties (relevant for the estimation of z) were estimated at ∼10% and 10 degrees, respectively [70]. Simulations indicate that ignoring the presence of such calibration errors does not lead to significant bias in the estimation of the GW parameters, as long as the SNR is not very large [71]. However, data analysis models for GW analysis that marginalize over calibration uncertainties are now available [72] and routinely utilized for the actual analysis [10]. The additional calibration uncertainty increases the statistical uncertainty of the inferred parameters by a similar amount. In our case, the largest source of uncertainty would come from the amplitude calibration and thus on the determination of D_L for the GW sources. Assuming, naively, an ET uncertainty budget of ∼10%, we estimate a similar degradation of our inference over $\vec{\Omega}$.

We also ignored the effects of weak lensing. Weak lensing is a zero mean process [73]; thus, when averaging over thousands of sources, it will not induce an overall bias in the estimate of $\vec{\Omega}$. A proper account of the lensing uncertainty would lead to similar conclusions as for the detector calibration uncertainty.

Even with the caveats discussed above, our study shows that even considering exclusively information coming from GW alone (with no input from any EM association) ET is capable of fully probing the evolution of the Universe and determine the value of $\vec{\Omega}$ with reasonable accuracy. We emphasize that our results apply to a pure GW-based inference of $\vec{\Omega}$. A more accurate determination of $\vec{\Omega}$ from GW-EM joint detections may be possible; thus the results presented in this study should be regarded as a lower limit to what the actual potentiality of ET is as a cosmological probe. Nevertheless, we showed that GW alone can be a feasible complementary and cross-validating route to probe the dynamics of the Universe.

ACKNOWLEDGMENTS

This work benefitted from stimulating discussions and comments from Bangalore Sathyaprakash, Alberto Vecchio, John Veitch, Ilya Mandel and Christopher Berry. We thank the anonymous referees for their

comments and suggestions. The work was funded in part by a Leverhulme Trust research project grant. W. D. P. is funded by the program "Rientro dei Cervelli Rita Levi Montalcini." C. M. is supported by the Science and Technology Research Council (Grant No. ST/L000946/1).

APPENDIX: INFERENCE OF THE COSMOLOGICAL PARAMETERS IN THE PRESENCE OF CENSORED DATA

We want to infer the value of the cosmological parameters $\vec{\Omega} \equiv (H_0, \Omega_m, \Omega_\Lambda, \ldots)$ given a set of gravitational wave observations. Consider a catalog of gravitational wave events $\mathcal{E} \equiv \{\epsilon_1, \ldots, \epsilon_N\}$. Each event is defined as a stretch of data $d_i(t)$ given by the sum of noise $n_i(t)$ and a gravitational wave signal $h_i(\vec{\Theta}; t)$, where $\vec{\Theta}$ indicates the set of all parameters of the signal and such that the SNR ρ is greater than a given threshold $\rho_{\rm th}$.

The likelihood to observe the event ϵ_i is given by $p(\epsilon_i|\vec{\Theta}, \mathrm{S}, \rho_{\rm th}, \mathrm{I})$ where S is the signal model that relates the signal parameters $\vec{\Theta}$ to a gravitational wave signal h. The posterior distribution for the parameters in our signal model S comes from the application of Bayes' theorem

$$p(\vec{\Theta}|\epsilon_i, \mathrm{S}, \rho_{\rm th}, \mathrm{I}) \propto p(\vec{\Theta}|\mathrm{S}, \mathrm{I}) p(\epsilon_i|\vec{\Theta}, \mathrm{S}, \rho_{\rm th}, \mathrm{I}) \tag{A1}$$

where $p(\vec{\Theta}|\mathrm{S}, \mathrm{I})$ is the prior probability distribution for the parameters $\vec{\Theta}$. Given a certain cosmic coalescence rate $R(\vec{\Omega}, z)$, there will be a certain number $M \equiv M(\vec{\Omega}, z)$ of gravitational wave events that will *not* be registered as events since their SNR will be below the selected threshold. Nevertheless, they encode information regarding the Universe and they must be taken into account in our inference. The likelihood $\mathcal{L}_k^-$ for a nondetected event ϵ_k^- is given by

$$\mathcal{L}_k^-(\epsilon_k^-, \rho_{\rm th}) \equiv p(\epsilon_k^-|\vec{\Omega}, R(\vec{\Omega}, z), \rho_{\rm th}, \mathrm{I}) \tag{A2}$$

$$= \int_0^{\rho_{\rm th}} p(\epsilon_k^-, \rho_k|\vec{\Omega}, R(\vec{\Omega}, z), \rho_{\rm th}, \mathrm{I}) \mathrm{d}\rho_k. \tag{A3}$$

For a set of M nondetected events, the likelihood will be given by

$$\mathcal{L}^-(\epsilon^-, \rho_{\rm th}) = \prod_{k=1}^{M} \mathcal{L}_k^-(\epsilon_k^-, \rho_{\rm th}) \tag{A4}$$

$$= [\mathcal{L}_k^-(\epsilon_k^-, \rho_{\rm th})]^M. \tag{A5}$$

The number of nondetected events $M(\vec{\Omega}, z)$ is a nuisance parameter which depends on $\vec{\Omega}$; the rate $R(\vec{\Omega}, z)$; the detection threshold $\rho_{\rm th}$; the observation time T; and the observed volume $V(\vec{\Omega}, \rho_{\rm th})$ as

$$M(\vec{\Omega}, z) = R(\vec{\Omega}, z) V(\vec{\Omega}, \rho_{\rm th}) T - N. \tag{A6}$$

We are now in the position of writing the posterior distribution for the cosmological parameters $\vec{\Omega}$:

$$\begin{aligned} p(\vec{\Omega}|\mathcal{E}, N, \rho_{\rm th}, S, \mathrm{I}) &\propto p(\vec{\Omega}|S, \mathrm{I}) \\ &\times \int_0^{R_{\rm max}(\vec{\Omega}, z)} \mathrm{d}R(\vec{\Omega}, z) p(R(\vec{\Omega}, z)|\vec{\Omega}, S, \mathrm{I}) \\ &\times \prod_{i=1}^{N} \mathcal{L}(\epsilon_i, \vec{\Omega}) \sum_{M=0}^{\infty} [\mathcal{L}_k^-(\epsilon_k^-, \rho_{\rm th})]^M p(M|\vec{\Omega}, R(\vec{\Omega}, z), \rho_{\rm th}). \end{aligned} \tag{A7}$$

It is interesting to verify that Eq. (A7) reduces to Eq. (10) in the limit of $\rho_{\rm th} \to 0$. In this limit we have also

$$M \to 0 \tag{A8}$$

$$p(M|\vec{\Omega}, R(\vec{\Omega}, z), \rho_{\rm th}) \to \delta_{M,0} \tag{A9}$$

$$\int_0^{\rho_{\rm th}} p(\epsilon_k^-, \rho_k|\vec{\Omega}, R(\vec{\Omega}, z), \rho_{\rm th}, \mathrm{I}) \mathrm{d}\rho_k \to 0. \tag{A10}$$

Therefore the term

$$[\mathcal{L}_k^-(\epsilon_k^-, \rho_{\rm th})]^M \to 1 \tag{A11}$$

and the nondetection part of the likelihood reduces to

$$\sum_{M=0}^{\infty} \delta_{M,0} = 1. \tag{A12}$$

Assuming that the rate $R(\vec{\Omega}, z)$ is given by the integral of Eq. (12), we recover the form of the likelihood (10) which we used in our study.

[1] http://www.ligo.caltech.edu/advLIGO/.
[2] B. P. Abbott *et al.* (LIGO Scientific Collaboration, Virgo Collaboration), Phys. Rev. Lett. **116**, 131103 (2016).
[3] http://wwwcascina.virgo.infn.it/advirgo/.
[4] K. Kuroda (LCGT Collaboration), Classical Quantum Gravity **27**, 084004 (2010).
[5] C. S. Unnikrishnan, Int. J. Mod. Phys. D **D22**, 1341010 (2013).
[6] B. P. Abbott *et al.* (LIGO Scientific Collaboration, Virgo Collaboration), Phys. Rev. Lett. **116**, 061102 (2016).
[7] B. P. Abbott *et al.* (LIGO Scientific Collaboration and Virgo Collaboration), Phys. Rev. Lett. **116**, 241103 (2016).
[8] B. P. Abbott, R. Abbott, T. D. Abbott, M. R. Abernathy, F. Acernese, K. Ackley, C. Adams, T. Adams, P. Addesso, R. X. Adhikari *et al.*, Phys. Rev. X **6**, 041015 (2016).
[9] B. P. Abbott *et al.* (LIGO Scientific Collaboration, Virgo Collaboration), Phys. Rev. Lett. **116**, 221101 (2016).
[10] B. P. Abbott *et al.* (LIGO Scientific Collaboration, Virgo Collaboration), Phys. Rev. Lett. **116**, 241102 (2016).
[11] B. P. Abbott *et al.* (LIGO Scientific Collaboration, Virgo Collaboration), Astrophys. J. **818**, L22 (2016).
[12] B. P. Abbott *et al.* (LIGO Scientific Collaboration, Virgo Collaboration), Astrophys. J. **833**, L1 (2016).
[13] J. Abadie, B. P. Abbott, R. Abbott, M. Abernathy, T. Accadia, F. Acernese, C. Adams, R. Adhikari, P. Ajith, B. Allen *et al.*, Phys. Rev. D **82**, 102001 (2010).
[14] W. Del Pozzo, J. Veitch, and A. Vecchio, Phys. Rev. D **83**, 082002 (2011).
[15] T. G. F. Li, W. Del Pozzo, S. Vitale, C. Van Den Broeck, M. Agathos, J. Veitch, K. Grover, T. Sidery, R. Sturani, and A. Vecchio, Phys. Rev. D **85**, 082003 (2012).
[16] N. Cornish, L. Sampson, N. Yunes, and F. Pretorius, Phys. Rev. D **84**, 062003 (2011).
[17] S. Nissanke, D. E. Holz, S. A. Hughes, N. Dalal, and J. L. Sievers, Astrophys. J. **725**, 496 (2010).
[18] W. Del Pozzo, Phys. Rev. D **86**, 043011 (2012).
[19] S. R. Taylor, J. R. Gair, and I. Mandel, Phys. Rev. D **85**, 023535 (2012).
[20] J. S. Read, C. Markakis, M. Shibata, K. Uryū, J. D. E. Creighton, and J. L. Friedman, Phys. Rev. D **79**, 124033 (2009).
[21] T. Hinderer, B. D. Lackey, R. N. Lang, and J. S. Read, Phys. Rev. D **81**, 123016 (2010).
[22] B. D. Lackey, K. Kyutoku, M. Shibata, P. R. Brady, and J. L. Friedman, Phys. Rev. D **89**, 043009 (2014).
[23] W. Del Pozzo, T. G. F. Li, M. Agathos, C. Van Den Broeck, and S. Vitale, Phys. Rev. Lett. **111**, 071101 (2013).
[24] M. Abernathy *et al.*, Tech. Rep. ET-0106A-10, 2011.
[25] A. Freise, S. Chelkowski, S. Hild, W. Del Pozzo, A. Perreca, and A. Vecchio, Classical Quantum Gravity **26**, 085012 (2009).
[26] M. Punturo *et al.*, Classical Quantum Gravity **27**, 194002 (2010).
[27] B. F. Schutz, Nature (London) **323**, 310 (1986).
[28] B. S. Sathyaprakash and B. F. Schutz, Living Rev. Relativ. **12**, 2 (2009).
[29] E. Nakar, A. Gal-Yam, and D. B. Fox, Astrophys. J. **650**, 281 (2006).
[30] B. S. Sathyaprakash, B. F. Schutz, and C. Van Den Broeck, Classical Quantum Gravity **27**, 215006 (2010).
[31] W. Zhao, C. van den Broeck, D. Baskaran, and T. G. F. Li, Phys. Rev. D **83**, 023005 (2011).
[32] S. Nissanke, D. E. Holz, N. Dalal, S. A. Hughes, J. L. Sievers, and C. M. Hirata, arXiv:1307.2638.
[33] B. D. Metzger, G. Martínez-Pinedo, S. Darbha, E. Quataert, A. Arcones, D. Kasen, R. Thomas, P. Nugent, I. V. Panov, and N. T. Zinner, Mon. Not. R. Astron. Soc. **406**, 2650 (2010).
[34] M. Tanaka, Adv. Astron. **2016**, 634197 (2016).
[35] K. Belczynski, R. O'Shaughnessy, V. Kalogera, F. Rasio, R. E. Taam, and T. Bulik, Astrophys. J. Lett. **680**, L129 (2008).
[36] C. L. MacLeod and C. J. Hogan, Phys. Rev. D **77**, 043512 (2008).
[37] A. Petiteau, S. Babak, and A. Sesana, Astrophys. J. **732**, 82 (2011).
[38] S. R. Taylor and J. R. Gair, Phys. Rev. D **86**, 023502 (2012).
[39] B. Sathyaprakash *et al.*, arXiv:1108.1423.
[40] C. Messenger and J. Read, Phys. Rev. Lett. **108**, 091101 (2012).
[41] T. G. F. Li, W. Del Pozzo, and C. Messenger, arXiv:1303.0855.
[42] B. P. Abbott, R. Abbott, T. D. Abbott, M. R. Abernathy, K. Ackley, C. Adams, P. Addesso, R. X. Adhikari, V. B. Adya, C. Affeldt *et al.*, arXiv:1607.08697.
[43] E. T. Jaynes, *Probability Theory: The Logic of Science* (Cambridge University Press, Cambridge, England, 2003).
[44] https://www.lsc-group.phys.uwm.edu/daswg/projects/lalsuite.html.
[45] B. Kiziltan, A. Kottas, and S. E. Thorsett, Bull. Am. Astron. Soc. **42**, 300.08 (2010).
[46] H. Müller and B. D. Serot, Nucl. Phys. **A606**, 508 (1996).
[47] B. D. Lackey, M. Nayyar, and B. J. Owen, Phys. Rev. D **73**, 024021 (2006).
[48] M. Prakash, J. R. Cooke, and J. M. Lattimer, Phys. Rev. D **52**, 661 (1995).
[49] D. M. Coward and R. R. Burman, Mon. Not. R. Astron. Soc. **361**, 362 (2005).
[50] D. W. Hogg, arXiv:astro-ph/9905116.
[51] E. V. Linder, Phys. Rev. Lett. **90**, 091301 (2003).
[52] T. Regimbau, T. Dent, W. Del Pozzo, S. Giampanis, T. G. F. Li, C. Robinson, C. Van Den Broeck, D. Meacher, C. Rodriguez, B. S. Sathyaprakash, and K. Wójcik, Phys. Rev. D **86**, 122001 (2012).
[53] C. Messenger and J. Veitch, New J. Phys. **15**, 053027 (2013).
[54] R. O'Shaughnessy, C. Kim, V. Kalogera, and K. Belczynski, Astrophys. J. **672**, 479 (2008).
[55] A. Buonanno, B. R. Iyer, E. Ochsner, Y. Pan, and B. S. Sathyaprakash, Phys. Rev. D **80**, 084043 (2009).
[56] C. K. Mishra, K. G. Arun, B. R. Iyer, and B. S. Sathyaprakash, Phys. Rev. D **82**, 064010 (2010).
[57] C. Markakis, J. S. Read, M. Shibata, K. Uryu, J. D. E. Creighton, and J. L. Friedman, arXiv:1008.1822.
[58] T. Damour, A. Nagar, and L. Villain, Phys. Rev. D **85**, 123007 (2012).
[59] S. Hild, S. Chelkowski, and A. Freise, arXiv:0810.0604.
[60] J. Skilling, in *Bayesian Inference and Maximum Entropy Methods in Science and Engineering: 24th International Workshop on Bayesian Inference and Maximum Entropy Methods in Science and Engineering, 2004, Garching, Germany*, edited by R. Fischer, R. Preuss, and U. von Toussaint, AIP Conf. Proc. No. 735 (AIP, New York, 2004), pp. 395–405.

[61] J. Veitch and A. Vecchio, Phys. Rev. D **81**, 062003 (2010).
[62] T. S. Ferguson, Ann. Stat. **1**, 209 (1973).
[63] *Bayesian Nonparametrics*, edited by N. L. Hjort, C. C. Holmes, P. Müller, and S. G. Walker (Cambridge University Press, Cambridge, 2010).
[64] D. M. Blei, M. I. Jordan *et al.*, Bayesian Analysis **1**, 121 (2006).
[65] http://code.google.com/p/haines/wiki/dpgmm.
[66] P. A. R. Ade, N. Aghanim, M. Arnaud, M. Ashdown, J. Aumont, C. Baccigalupi, A. J. Banday, R. B. Barreiro, J. G. Bartlett *et al.* (Planck Collaboration), Astron. Astrophys. **594**, A13 (2016).
[67] P. A. R. Ade, N. Aghanim, M. Arnaud, M. Ashdown, J. Aumont, C. Baccigalupi, A. J. Banday, R. B. Barreiro, N. Bartolo *et al.* (Planck Collaboration), Astron. Astrophys. **594**, A14 (2016).
[68] S. Vitale, R. Lynch, J. Veitch, V. Raymond, and R. Sturani, Phys. Rev. Lett. **112**, 251101 (2014).
[69] C. Messenger, K. Takami, S. Gossan, L. Rezzolla, and B. S. Sathyaprakash, Phys. Rev. X **4**, 041004 (2014).
[70] B. P. Abbott *et al.* (LIGO Scientific Collaboration), arXiv: 1602.03845.
[71] S. Vitale, W. Del Pozzo, T. G. F. Li, C. Van Den Broeck, I. Mandel, B. Aylott, and J. Veitch, Phys. Rev. D **85**, 064034 (2012).
[72] W. M. Farr, B. Farr, and T. Littenberg, Tech. Rep. LIGO Document T1400682-v1 2015.
[73] M. Bartelmann and P. Schneider, Phys. Rep. **340**, 291 (2001).